Asian Journal of Applied Science and Technology (AJAST)
(Open Access Quarterly International Journal) Volume 2, Issue 3, Pages 135-143, July-September 2018

CFD Analysis of Solar Air Heater Roughened with S-shape Ribs with Gap and S-shape Protrusion Roughness

Sumit Kumar[1] and Vijay Singh Bisht[2]

[1]*sumit.pce90@gmail.com, Faculty of Technology, Uttarakhand Technical University, Dehradun, India.*
[2]*vsinghbisht5@gmail.com, Faculty of Technology, Uttarakhand Technical University, Dehradun, India.*

Article Received: 20 April 2018 *Article Accepted: 29 July 2018* *Article Published: 24 August 2018*

ABSTRACT

The study presents a performance evaluation of a solar collector for heating air roughened with multiple broken arc shaped ribs combined with circular protrusion in arc shape on the back side of absorber plate. Simulation work has been carried out in ANSYS FLUENT (v14.0) platform with RNG k-Ɛ model at constant heat flux 1200 w/m2. In order to compare the thermal-hydraulic performance of the proposed design for a range of reynolds number (3000 to 18,000). A significant improvement is observed in Nusselt number at high Reynolds Number (above 8000).The rib roughness has relative roughness pitch of 12, 16, 20 and 24, height of broken arc rib is 1.6 mm. Further, the thermal efficiency, obtained in the present work has been compared with those obtained for other roughness geometries available in the literature for common roughness parameters and operating parameters to validate the results. It has been observed that above used geometry can significantly improve nusselt number in range (2.3-4.5¬) and friction factor value ranges from (1.3-3.8) in comparison with smooth duct. Value of friction factor has been reduced compared with other previous research work. The thermal hydraulic performance factor of solar air heater is 3.11.This new geometry increases nusselt number with very little increase in friction factor and hence longer life and more economical than previous geometries.

Keywords: Solar air heater, CFD, Nusselt Number.

1. INTRODUCTION

Energy is the one of the most important need of mankind, be it proving light or be it to run machines. Energy in different forms and functions has portrayed a very important role in the extensive economic boom and industrialization. For coming generations, we need to depend on the source which can provide infinite energy. Solar energy can be said to be one of those forms which is freely available, and easily accessible and of course is non-polluting in nature. It is considered to be an indispensable source of energy to meet the growing demand for the sustainable development and to control the global climate change. The need to enhance the thermal performance of heat exchangers, consequently, effecting energy, material, and cost savings as well as a consequential mitigation of environmental degradation had led to the development and use of many heat transfer enhancement techniques. There are several devices like solar water heater [1-2] and solar air heater [3-4] are used to harness the solar energy. Many researchers have conducted numerical study of solar air heater [5-9]. CFD is a vital tool to analyze thermal systems [10-11].

Kumar et.al [12] carried out 3D CFD investigation of solar air heater using broken curved ribs and concluded that these ribs augmented thermo-hydraulic performance. Gupta and Varshney [13] carried out CFD study of solar air heater, they concluded that by incorporation of sectioned tapered rib thermal performance of Solar air heater enhances. Gupta et.al [14] concluded that transverse ribs enhance the heat transfer rate of air flowing in solar air heater duct.

2.1 Objectives of Present Work

The objectives of the present work are shown as follows:

(1) To study the effect of variation in the Reynolds number (Re = 3000, 6000, 9000, 12000, 15000, 18000) on the fluid flow characteristics, heat transfer characteristics, and friction characteristics.

(2) To study the effect of variation in the dimple pitch height and boot shaped ribs distance (p/e = 12 – 24) and the fluid flow characteristics, heat transfer characteristics, and friction characteristics.

(3) To study the effect of variation in relative roughness height ($e/D_{h)}$ = 0.030.

3. METHODOLOGY

3.1 INTRODUCTION

The section represents the design and CFD analysis of a solar rectangular model which consist different roughened parts as S-shaped with gap and protrusion dimple roughness. The model of solar air heater is designed in 3-Dimensional form by software Ansys workbench. Ansys fluent provides dealing with all modeling in case of any type of working fluid can be accomplished. Analysis of the rectangular channel was done by Computational fluid dynamics (CFD) and the design is taken in the form of 3-Dimensional CFD.

In the section CFD is used for calculation of the construction of the model and is devoted to solve the all types of the energy equation. The study of the model created to analyse the working fluid flow as air and heat transfer enhancement characteristics in a rectangular duct with different variation in the combination of S-shaped and protrusion dimple ribs roughness. Here, the selection of suitable turbulence model made on the basis of the literature survey and experimental research paper. The computational processes in solving the simulation using the ANSYS-CFD are presented in the following subsections.

This model is used to define the condition of heat transfer and friction factor in the solar Rectangular channel. The some parameters had taken from validated paper V-shaped, Multi v-shaped, and Multi v-shaped with gap geometries roughness which contain Heat transfer, friction factor, solar air heater, CFD, artificial roughness presented by Ravendra Kumar Ray and Dr. A. R. Jaurker.

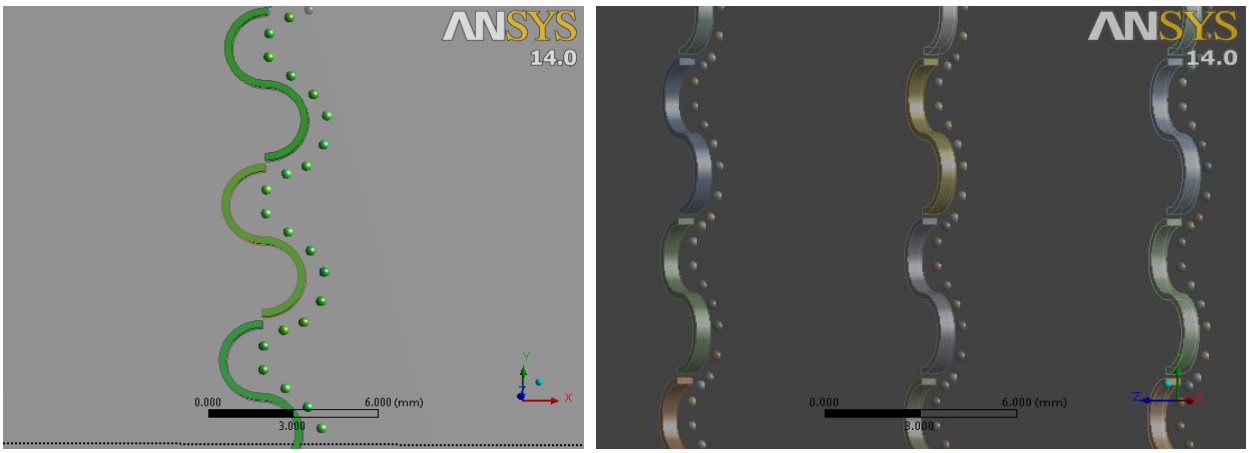

Figure 3.1 Design of the combination of Continuous S – shaped with gap roughness and Protrusion dimple shaped roughness.

 Online ISSN: 2456-883X

3.2 PARAMETERS

S. NO.	PARAMETERS	RANGE OF VALUES
1	Rectangular channel Total Length, L	1500 mm
2	Channel Entrance Length, L1 Channel Test Length, L2 Channel Exit Length, L3	400 mm 900 mm 200 mm
3	Channel Width, W	200 mm
4	Channel Height, H	30 mm
5	Relative Roughness Pitch, p/e	12, 16, 20, and 24
6	Hydraulic Diameter, D_h	52.18
7	Relative Hydraulic Diameter Ratio , e/D_h	0.030
8	Roughness ribs Height, e	1.6 mm
9	Uniform Heat Flux, I	1200 w/m^2
10	Reynolds Number, Re	3000, 6000, 9000, 12000, 15000 and 18000
11	Pitch space between the continuous S-shaped with protrusion dimple rib Roughness, P	19.2, 25.6, 32 and 38.4
12	Diameter of the protrusion dimple shaped, D_p	0.3 mm and 0.5
13	Space pitch between the protrusion dimple Shaped, P_d	0.7 mm
14	Prandtl Number, Pr	0.707
15	Width of the continuous S-shaped roughness rib, w	40 mm
16	Relative channel width to S-shaped rib width ratio, W/w	5
17	Gap between the S-shape and protrusion dimple, G_{sp}	0.5 mm and 1.5 mm
18	Gap between the continuous s-shaped, g	0.6 mm

In the solar rectangular duct quadrilaterals and hexahedral meshing is used, quadrilateral for Protrusion dimple and hexahedral for s-shaped with gap roughness. When adaption is employed appropriately the resulting mesh is most favourable for the flow solution. Thus, to avoid wastages of the computational resources the addition of unnecessary cells was stopped. As shown in table after 796554 numbers of cells and number of nodes are used

236789, the variation in the value of heat transfer is negligible. The grid independence table 3.2 shows the perfect number of cells and nodes where the variation in the Nusselt number is negligible.

3.3 Grid Independent Test

S. No.	Number of nodes	Number of cells	Nusselt number
1	156648	456447	58.9592
2	197065	780990	79.0655
3	276789	1296554	38.3556
4	312344	1567677	38.9577

3.4.1 Continuity equation

The mathematical expression of the principle of conservation of mass applied to an elemental control volume within a fluid under motion is known as continuity equation and is given by:

$$\frac{\partial \vec{u}}{\partial x} + \frac{\partial \vec{v}}{\partial y} + \frac{\partial \vec{w}}{\partial z} = 0 \qquad (3.1)$$

This is the mass continuity equation for three - dimensional steady flow fluid and it has no breaks in it.

3.4.2 Momentum equation

It is based on law of conservation of moment or on momentum principle for turbulent flow field, which state that the net force acting on a mass acceleration fluid equal to the change in momentum of flow per unit time in the direction.

X- Momentum equations:

$$\left(\vec{u}\frac{\partial \vec{u}}{\partial x} + \vec{v}\frac{\partial \vec{u}}{\partial y} + \vec{w}\frac{\partial \vec{u}}{\partial z}\right) = -\frac{1}{\rho}\frac{\partial p}{\partial x} + v\left(\frac{\partial^2 \vec{u}}{\partial x^2} + \frac{\partial^2 \vec{u}}{\partial y^2} + \frac{\partial^2 \vec{u}}{\partial z^2}\right) \qquad (3.2)$$

Y- Momentum equation:

$$\left(\vec{u}\frac{\partial \vec{v}}{\partial x} + \vec{v}\frac{\partial \vec{v}}{\partial y} + \vec{w}\frac{\partial \vec{v}}{\partial z}\right) = -\frac{1}{\rho}\frac{\partial p}{\partial y} + v\left(\frac{\partial^2 \vec{v}}{\partial x^2} + \frac{\partial^2 \vec{v}}{\partial y^2} + \frac{\partial^2 \vec{v}}{\partial z^2}\right) \qquad (3.3)$$

Z – Momentum equations:

$$\left(\vec{u}\frac{\partial \vec{v}}{\partial x} + \vec{v}\frac{\partial \vec{v}}{\partial y} + \vec{w}\frac{\partial \vec{v}}{\partial z}\right) = -\frac{1}{\rho}\frac{\partial p}{\partial z} + v\left(\frac{\partial^2 \vec{v}}{\partial x^2} + \frac{\partial^2 \vec{v}}{\partial y^2} + \frac{\partial^2 \vec{v}}{\partial z^2}\right) \qquad (3.4)$$

3.4.3 Energy equation

Assuming that the flow is steady and incompressible with constant thermal conductivity no compression work and without heat generation for steady turbulent flow:

In this case no viscous heating,

$$\vec{u}\frac{\partial t}{\partial x} + \vec{v}\frac{\partial t}{\partial y} + \vec{w}\frac{\partial t}{\partial y} = \alpha\left(\frac{\partial^2 t}{\partial x^2} + \frac{\partial^2 t}{\partial y^2} + \frac{\partial^2 t}{\partial y^2}\right) \qquad (3.5)$$

3.5 Validation

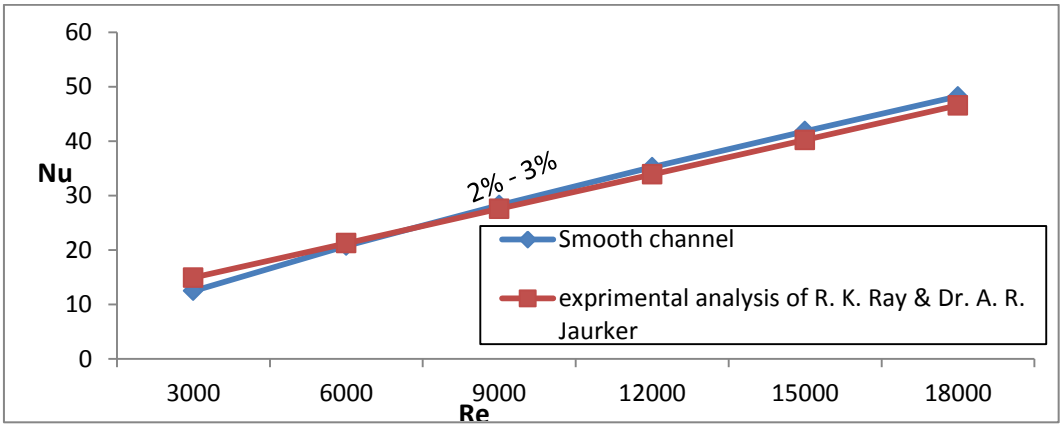

Figure 3.2 Validation with Experimental research paper results of Ravendra Kumar Ray and Dr. A. R. Jaurker.

4. RESULTS AND DISCUSSION

4.1 VELOCITY CONTOUR

Velocity contour in presented by the help of Ansys fluent workbench which is performed in the form of graph after conclusion the numerical investigation of the designer of the solar absorber rectangular plate. The velocity contour is a verification method of the average velocity of the working fluid flowing in the designed rectangular channel and the velocity of the working fluid as air circulated around the cross sectional area of the solar air heater.

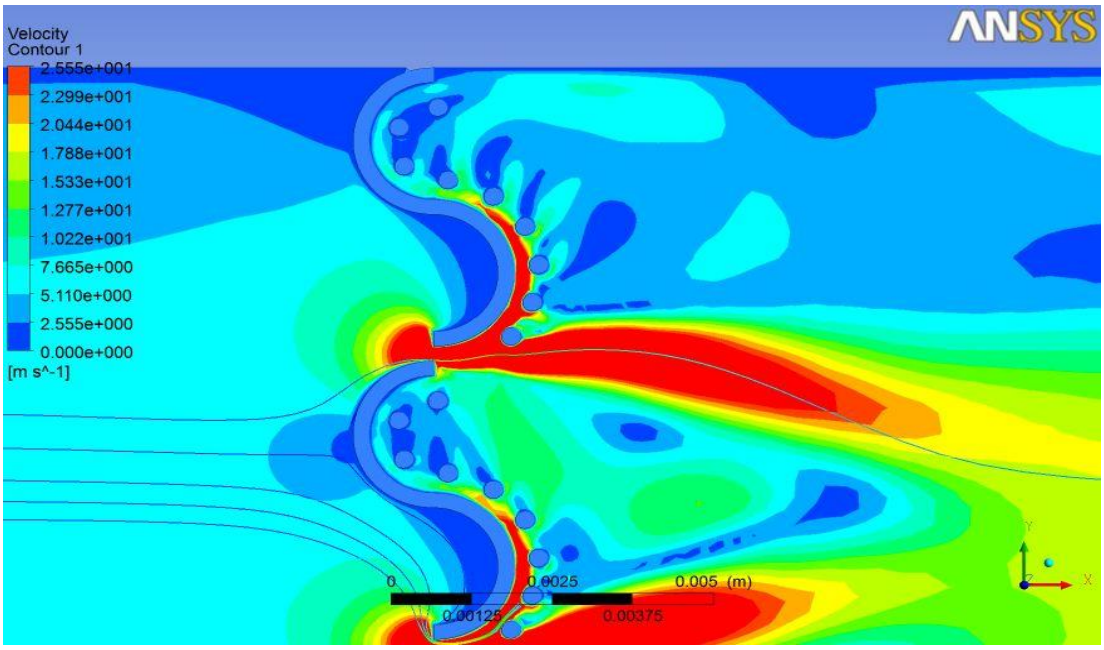

Figure 4.1 Variation in the velocity contour

The figure 4.1 shows the variation in the velocity contour with respect to the variation in the parameters. There are number of parameters used to examine the contour graph when contour required explaining the number of variation like variation in the Reynolds number. The figure shows the change in the velocity of air at the gap g = 0.6 mm taken between the continuous s-shape, the gap g = 0.6 mm is a more desired part of the solar absorber plate to

passes the air and circulation around the surface. We can see that reattachment zone is a mixing flow of the warm and cool air as upward and downward flow. The upward and downward reattachment zone calculate the heat transfer characteristic at space between the s-shaped with gap and between the protrusion dimple G_{sp} = 0.5 mm and protrusion dimple D_p = 0.3 mm. the velocity changes from 0 m/s to 25.55 m/s at Reynolds number Re = 18000 and more successful relative roughness pitch p/e = 20.

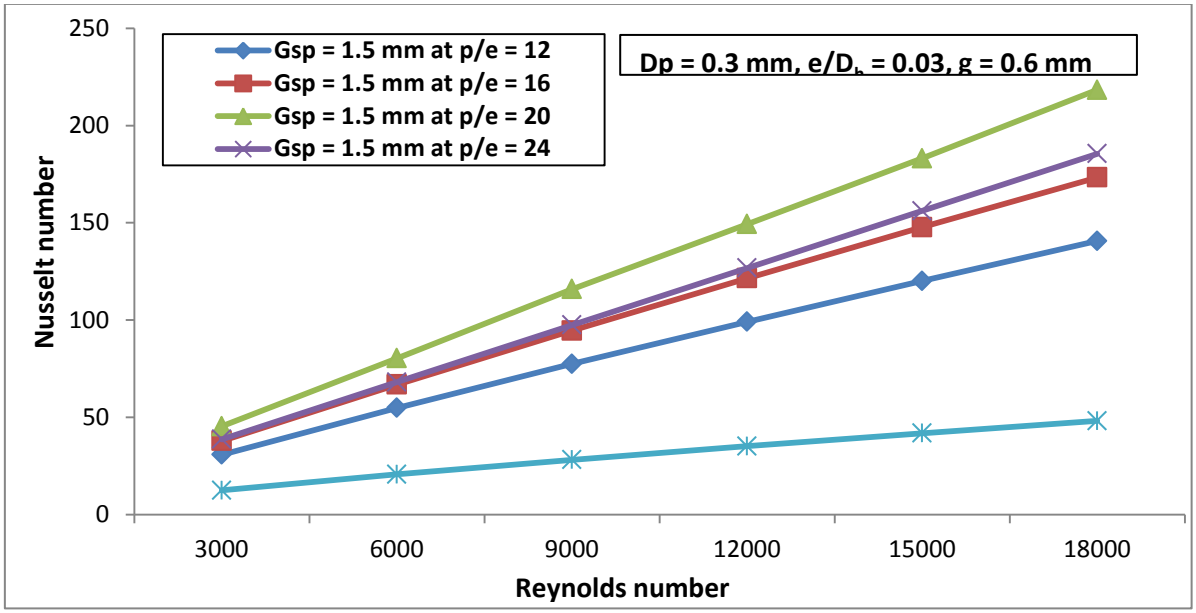

Figure 4.2 shows the variation in the Nusselt number with respect to the Reynolds number

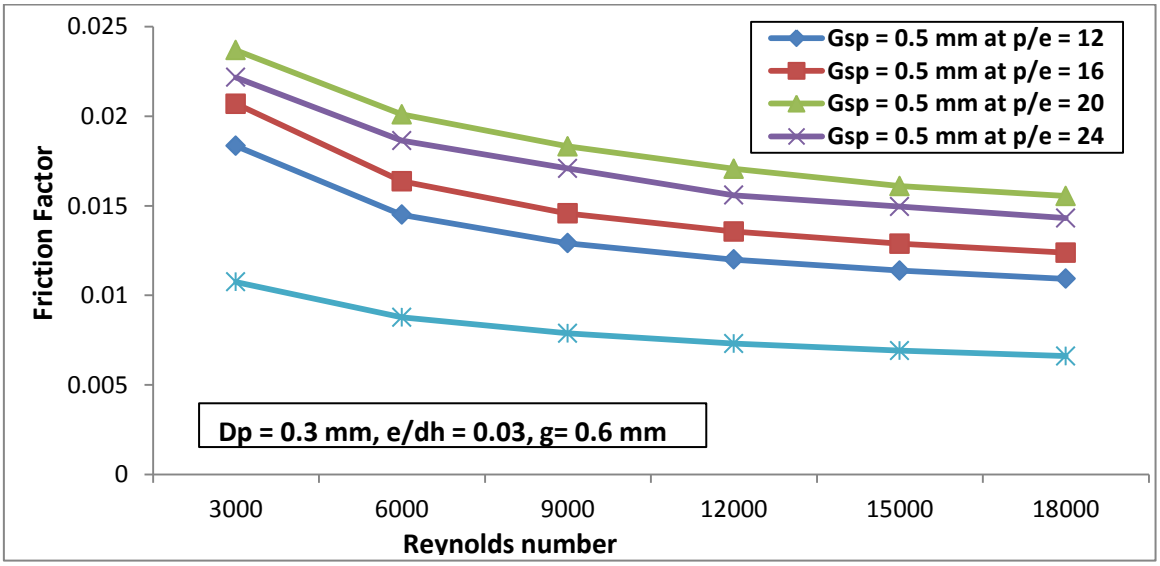

Figure 4.3 shows the variation in the friction factor with respect to the Reynolds number Re = 3000 – 18000

This figure 4.2 shows the comparison between the Nusselt number and Reynolds number Re = 3000 – 18000. In this figure can see that the maximum Nusselt number of the solar rectangular channel Nu = 218.2725 is obtained when the space between the s-shaped with gap g = 0.6 mm and protrusion dimple increase Gsp = 1.5 mm at diameter of the protrusion dimple Dp = 0.3 mm and relative pitch roughness p/e = 20, at p/e = 12 we obtained

Online ISSN: 2456-883X

minimum Nusselt number Nu = 140.6336 at same fixed values given in the figure, at relative pitch roughness p/e = 16 the Nusselt number is Nu = 173.348, at relative pitch roughness, p/e = 24 the maximum nusselt number starts to decrease and finally achieved Nu = 185.45796. These results of the inserted roughness parts in the smooth solar rectangular channel also compared with smooth rectangular channel and in case of smooth channel the Nusselt number is Nu = 48.23088.

In this figure 4.3 the comparison between the friction factor and Reynolds number Re = 3000 – 18000 for the variation in the relative pitch roughness p/e = 12, 16, 20, and 24. In the figure can see that the friction factor increasing with increasing in the relative pitch roughness (p/e = 12) because less reattachment zone deform around the roughness and low heat transfer generated in the region and another section low Reynolds number (Re = 3000) where friction factor increased the main reason is low velocity or recirculation of warm air around the surface due to the problem air is trapped and produced high stress in the designed part. The maximum friction factor Fr = 0.01554118 at relative pitch roughness p/e = 20 the space between s-shaped with gap, g = 0.6 mm and protrusion dimple Dsp = 0.5 mm and diameter of the protrusion dimple Dp = 0.3 mm, and at p/e = 12 the minimum friction factor Fr = 0.01092649 at the same space Dsp = 0.5 mm and diameter of the protrusion Dp = 0.3 mm, at p/e = 16 the friction factor Fr = 0.01237849 and at p/e = 24 the friction factor Fr = 0.01431569 starts to decrease with compare to the p/e = 20. All the results are compared with smooth friction factor Fr = 0.00660241.

4.4 Thermal hydraulic performance

The thermal hydraulic performance so solar absorber channel in which roughness is used based on the working fluid as air velocity and temperature. The thermal performance is increased with turbulence of the working fluid and Thermal hydraulic performance is given by the scientific researcher Webb and Eckert.

$$\eta = \frac{(Nu_r/Nu_s)}{(f_r/f_s)^{\frac{1}{3}}} \qquad (4.1)$$

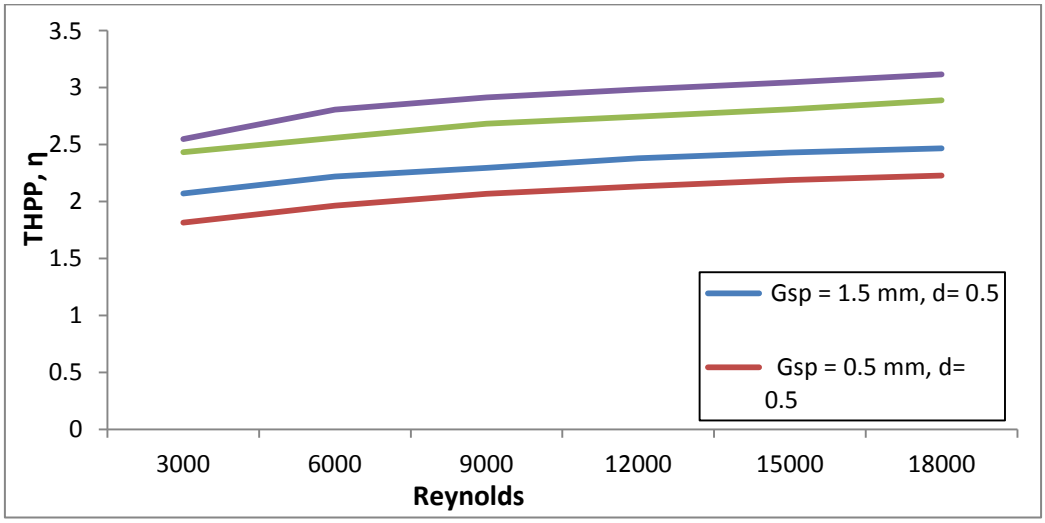

Figure 4.4 shows the variation in the thermal hydraulic performance with respect to the Reynolds number

 Online ISSN: 2456-883X

5. CONLUSION

The following conclusions have been examined on the basis of the given numerical investigation.

1. The presented results calculated from the designed solar absorber rectangular channel which is based on the k-e turbulent model. This k-e model is more effective near the wall and around the roughness to calculate and capture the successfully heat transfer and friction characteristic surface area of the solar air heater.

2. The introduction of the rectangular channel with artificial roughness enhances the heat transfer and friction factor coefficient compared with smooth channel.

3. The heat transfer rate increased and friction factor decreased with increased in the Reynolds number with respect to the various values of the parameters.

4. The maximum Nusselt number Nu = 218.2725 is obtained at relative pitch roughness p/e = 20, space between the s-shaped with gap g = 0.6 mm and protrusion roughness Gsp = 1.5, diameter of the protrusion roughness Dp = 0.3 mm and Reynolds number Re = 18000.

5. The minimum friction Fr = 0.00872538 is examined at the relative pitch roughness p/e = 12, space between the s-shaped with gap g = 0.6 mm and protrusion dimple Gsp = 0.5 mm and diameter of the protrusion roughness Dp = 0.5 mm and Reynolds number Re = 18000.

6. The heat transfer rate as Nusselt number increased in the range of 2.3 – 4.5 times as compared to smooth channel and the friction factor increased 1.3 – 3.8 times as compared to the smooth duct.

7. The maximum thermal hydraulic performance $\eta = 3.11747136$ obtained at the space between the s-shaped with gap g = 0.6 mm and protrusion roughness $G_{sp} = 1.5$ mm and Diameter of the protrusion roughness $D_p = 0.3$ mm.

REFERENCES

1. Prabhakar Bhandari, Lokesh Varshney, Vijay Singh Bisht (2018). Numerical analysis of Hybrid Solar Water Heating System Using Wire Screen Packed Solar Air Heater. 1st International Conference on New Frontiers in Engineering, Science & Technology, vol 1, pp 415-1422.
2. L Varshney, Prabhakar Bhandari, Vijay Singh Bisht(2014).Performance Evaluation of Hybrid Solar Water Heating System Using Wire Screen Packed Solar Air Heater**.** Int. Journal of Engineering Research and Application (IJERA) 311-316.
3. Bisht, V. S., Patil, A. K., & Gupta, A. (2018). Review and performance evaluation of roughened solar air heaters. Renewable and Sustainable Energy Reviews, *81*, 954-977.
4. Gangwar, H.P, Rawat, K.S & Pratihar , A.K (2018). Heat Transfer Studies in an artificial roughened solar air heater having wire rib roughness. International journal of Pure and Applied Mathematics, 119, 1505-1509.
5. Ankit Kumar, Vijay Singh Bisht, Maneesh Khati, and Satish Kumar*(2017).*Numerical Study of a Roughened Solar Air Heater using Matlab, *IJIACE,4.*
6. Akbarzadeh, M., Rashidi, S., Karimi, N., & Ellahi, R. (2018). Convection of heat and thermodynamic irreversibilities in two-phase, turbulent nanofluid flows in solar heaters by corrugated absorber plates. Advanced Powder Technology**.**

7. Soi, A., Singh, R., & Bhushan, B. (2018). Heat transfer and friction characteristics of solar air heater duct having protruded roughness geometry on absorber plate. Experimental Heat Transfer, 1-15.

8. Singh, I., & Singh, S. (2018). CFD analysis of solar air heater duct having square wave profiled transverse ribs as roughness elements. Solar Energy, *162*, 442-453.

9. Rashidi, S., Javadi, P., & Esfahani, J. A. (2018). Second law of thermodynamics analysis for nanofluid turbulent flow inside a solar heater with the ribbed absorber plate. Journal of Thermal Analysis and Calorimetry, 1-13.

10. Akbarzadeh, M., Rashidi, S., Karimi, N., & Omar, N. (2018). First and second laws of thermodynamics analysis of nano fluid flow inside a heat exchanger duct with wavy walls and a porous insert. Journal of Thermal Analysis and Calorimetry, 1-18.

11. Kumar, S., & Bisht, V. S. (2018). 2D Modelling and Simulation of Heat Transfer in Blast Furnace Hearth Using ANSYS. In *Intelligent Communication, Control and Devices* (pp. 1051-1063). Springer, Singapore.

12. Kumar, K., Kaushik, S., & Bisht, V. S(2017). CFD Analysis on Solar Air Heater with Artificial Roughned Broken Curved Ribs,8,264-275.

13. Gupta, A. D., & Varshney, L. (2017). Performance prediction for solar air heater having rectangular sectioned tapered rib roughness using CFD. Thermal Science and Engineering Progress, *4*, 122-132.

14. Gupta, A. D., Varshney, L., & Pratihar, A. K. (2016). Heat Transfer and Pressure Drop Characteristics In A Duct With Roughened Absorber Plate Having Rectangular Transversed Rib Using ANSYS. Int. J. Sci. Eng. Res., 7, 252-264.